Sequence motifs of tissue inhibitor of metalloproteinases 2 (TIMP-2) determining progelatinase A (proMMP-2) binding and activation by membrane-type metalloproteinase 1 (MT1-MMP)

Joanna R. WORLEY*, Philip B. THOMPKINS†[1], Meng H. LEE*[1], Mike HUTTON*, Paul SOLOWAY‡, Dylan R. EDWARDS*, Gillian MURPHY*[2,3] and Vera KNÄUPER†[3]

*School of Biological Sciences, University of East Anglia, Norwich NR4 7TJ, U.K., †Biomedical Tissue Research, Department of Biology, University of York, York YO10 5YW, U.K., and ‡Cornell University, Division of Nutritional Sciences, 108 Savage Hall, Ithaka, NY 14853, U.S.A.

Fundamental cellular processes including angiogenesis and cell migration require a proteolytic cascade driven by interactions of membrane-type matrix metalloproteinase 1 (MT1-MMP) and progelatinase A (proMMP-2) that are dependent on the presence of tissue inhibitor of metalloproteinases 2 (TIMP-2). There are unique interactions between TIMP-2 and MT1-MMP, which we have previously defined, and here we identify TIMP-2 sequence motifs specific for proMMP-2 binding in the context of its activation by MT1-MMP. A TIMP-2 mutant encoding the C-terminal domain of TIMP-4 showed loss of proMMP-2 activation, indicating that the C-terminal domain of TIMP-2 is important in establishing the trimolecular complex between MT1-MMP, TIMP-2 and proMMP-2. This was confirmed by analysis of a TIMP-4 mutant encoding the C-terminal domain of TIMP-2, which formed a trimolecular complex and promoted proMMP-2 processing to the intermediate form. Mutants encoding TIMP-4 from Cys^{1} to Leu^{185} and partial tail sequence of TIMP-2 showed some gain of activating capability relative to TIMP-4. The identified residues were subsequently mutated in TIMP-2 (E^{192}–D^{193} to I^{192}–Q^{193}) and this inhibitor showed a significantly reduced ability to facilitate proMMP-2 processing by MT1-MMP. Furthermore, the tail-deletion mutant $\Delta_{186-194}$TIMP-2 was completely incapable of promoting proMMP-2 activation by MT1-MMP. Thus the C-terminal tail residues of TIMP-2 are important determinants for stable trimolecular complex formation between TIMP-2, proMMP-2 and MT1-MMP and play an important role in MT1-MMP-mediated processing to the intermediate and final active forms of MMP-2 at the cell surface.

Key words: activation, murine tissue inhibitor of metalloproteinases 4 (TIMP-4), site-directed mutagenesis, trimolecular complex.

INTRODUCTION

Matrix metalloproteinases (MMPs) are a family of zinc endopeptidases that play critical roles in extracellular matrix remodelling in development and disease [1,2]. Two recent gene-ablation studies have shown that angiogenesis is mediated by membrane-type MMP 1 (MT1-MMP) and MMP-2 [3,4], leading to the development of tissue inhibitor of metalloproteinase (TIMP)-based strategies such as anti-cancer gene therapeutics (reviewed in [5]). Four TIMPs have now been cloned, each representing proteins of around 190 amino acid residues [6–9] The inhibitory features of TIMP-1, -2 and -3 have been well characterized and they inhibit most members of the MMP family with low inhibition constants (reviewed in [10]). However, they show variations in their affinity for different MMPs due to differences in their ability to interact with the catalytic domain, e.g. MT1-MMP, MT2-MMP and MT5-MMP are only poorly inhibited by TIMP-1 [11].

TIMP-4 is the most recent member of the TIMP family and two initial studies have provided some insight into its specificity for individual MMPs [12,13]. It has been shown that TIMP-4 binds to progelatinase A (proMMP-2) via the C-terminal domain of the enzyme [13,14]. However, unlike TIMP-2, TIMP-4 is unable to promote proMMP-2 activation by MT1-MMP [14–16]. ProMMP-2 activation is thought to be dependent on the establishment of an 'MT1-MMP/TIMP-2' receptor, which mediates proMMP-2 binding through C-terminal-domain interactions, forming a trimolecular complex at the cell surface. An adjacent inhibitor-free MT1-MMP molecule is involved in stepwise proteolytic processing of proMMP-2 to an intermediate form, which then undergoes auto proteolysis, generating the fully active enzyme which is released from the cell membrane [17–20]. *TIMP-2*$^{-/-}$ mice were shown to be deficient in proMMP-2 activation by MT1-MMP *in vivo* [21,22], suggesting that TIMP-2 is unique amongst the TIMPs in promoting proMMP-2 activation at low inhibitor concentrations.

Abbreviations used: MMP, matrix metalloproteinase; MT1-MMP, membrane-type MMP 1; catMT1-MMP, haemopexin domain deletion mutant of MT1-MMP with residues 269–559 deleted; proMMP-2, progelatinase A; $proE^{375} \rightarrow A$ MMP-2, $E^{375} \rightarrow A$ inactive point mutant of proMMP-2; TIMP, tissue inhibitor of metalloproteinases; N-TIMP-4, N-terminal TIMP-4 residues 129–195 deleted; N-TIMP-2, N-terminal TIMP-2 residues 128–194 deleted; N-TIMP-4:C-TIMP-2, TIMP-4 residues 1–128:TIMP-2 residues 128–194; $\Delta_{186-194}$TIMP-2, tail-deletion mutant of TIMP-2 with residues 186–194 deleted; N-TIMP-2:C-TIMP-4, TIMP-2 residues 1–127:TIMP-4 residues 129–195; TIMP-4:TIMP-$2^{K185-P194}$, TIMP-4 with tail-sequence residues 185–194 from TIMP-2; TIMP-4:TIMP-$2^{Y178-P184}$, TIMP-4 with tail-sequence residues 178–184 from TIMP-2; TIMP-4:TIMP-$2^{E192-D193}$, TIMP-4 with tail-sequence residues 192–193 from TIMP-2; IQ-TIMP-2, TIMP-2 with tail-sequence residues I^{192}–Q^{193} from TIMP-4; $proE^{375} \rightarrow A$ MMP-2–TIMP-2, bimolecular complex between $proE^{375} \rightarrow A$ MMP-2 and TIMP-2; SL, stromelysin-1; proMMP-2-C-SL, proMMP-2 mutant encoding the C-terminal domain of SL residues 248–460; proMMP-2-C-SLGLGL, proMMP-2 mutant encoding C-terminal domain residues 248–305 from SL and residues 475–631 from MMP-2; proMMP-2-C-SLGLSL, proMMP-2 mutant encoding C-terminal domain residues 248–305 and 400–460 from SL and residues 475–567 from MMP-2.

[1] These authors contributed equally to this work.

[2] Present address: University of Cambridge, Department of Oncology, Cambridge Institute for Medical Research, Hills Road, Cambridge CB2 2XY, U.K.

[3] To whom correspondence should be addressed (e-mail vk8@york.ac.uk and gm290@cam.ac.uk).

© 2003 Biochemical Society

Table 1 Summary of oligonucleotides used to create mouse TIMP-4 mutants

Mutations are described in the text. Underlined residues: primer 1, *Nde*I site; primer 2, stop codon and *Eco*RI site.

Mutation	Oligonucleotide no.	Oligonucleotide sequence
N-TIMP-4	1	5′-CCCTGGACGGGGTCATATGTGCAGCTGTGCGCCTG-3′
	2	5′-GGAATTCCCTAGCCACAGTTCGGTGGTAGTGATG-3′
N-TIMP-2:C-TIMP-4	3	5′-GATTTGGCACTCGCACCCATCTGGTACCTGTGGTTC-3′
	4	5′-GGGTGCGAGTGCCAAATCACCACTTGCTATGCA-3′
N-TIMP-4:C-TIMP-2	5	5′-AGCCTGAATCATCACTACCACCAGAACTGTGGCTGCAAGATCACGCGCTGCCCCATGATCCCGTGCTACAT-3′
TIMP-4:TIMP-2$^{K185-P194}$	6	5′-GCTGGTACCGAGGCCACCTACACCTCAAGCAGGAGTTTCTCGACATCGAGGACCCATAATCTAGA-3′
	7	5′-AGCTTCTAGATTATGGGTCCTCGATGTCGAGAAACTCCTGCTTGAGGTGTAGGTGGCGTCGGTACCAGCTGCA-3′
TIMP-4:TIMP-2$^{Y178-P184}$	8	5′-GCTGGTACCGCGGCGCGGCGCCCCCCCGGAAGGAGTACGTTGACATCATCCAGCCCTAATCTAGA-3′
	9	5′-AGCTTCTAGATTAGGGCTGGATGATGTCAACGTACTCCTTCCGGGGGGGCGCCGCGCCGCGGTACCAGCTGCA-3′
TIMP-4:TIMP-2$^{E192-D193}$	10	5′-GCTGGTACCGAGGCCACCTACACCTCCGGAAGGAGTACGTTGACATCGAAGATCCCTAGTCTAGA-3′
	11	5′-AGCTTCTAGACTAGGGATCTTCGATGTCAACGTACTCCTTCCGGAGGTGTAGGTGGCCTCGGTACCAGCTGCA-3′
IQ-TIMP-2	12	5′-CCCAAGCTTATGGTTGGATGATGTCGAGAAACTCCTGCTTGGGGGGCGCC-3′

We have demonstrated previously that the C-terminal domain of TIMP-2 is required for efficient interaction with both pro- and active MMP-2 [23]. In contrast, the C-terminal domain of TIMP-2 showed no significant interaction with MT1-MMP. However, we were able to define a highly specific N-terminal-domain interaction involving the residue Tyr^{36}. Substitution of this residue with glycine resulted in a 40-fold increase of the K_i^{app} for MT1-MMP, but had no effect on the TIMP-2/MMP-2 rate of binding. It might be speculated that their respective N-terminal domains mainly govern the MT1-MMP–TIMP-2 interactions, while their C-terminal domains rule the proMMP-2–TIMP-2 interactions. In view of these specialized interactions between the members of the trimolecular complex, TIMP-2, proMMP-2 and MT1-MMP, we set out to determine the sequence requirements for TIMP-2-dependent proMMP-2 activation by MT1-MMP at the molecular level.

This was achieved by analyses of site-directed mutants derived from murine TIMP-4 and human TIMP-2 in solution and using a cellular model system established from *TIMP-2*$^{-/-}$ cells. We report gain and loss of function of murine TIMP-4 or human TIMP-2 mutants, and identify residues that are important for trimolecular complex formation and proMMP-2 activation. The implications of our findings are discussed in the light of the recently published X-ray crystal structure analysis of the proMMP-2–TIMP-2 complex [24]. Our data represent the basis of future work to engineer TIMP-2 mutants that are capable of preventing proMMP-2 activation by MT1-MMP at the cell surface.

EXPERIMENTAL

Preparation of murine TIMP-4 and human TIMP-2 mutants

An *Escherichia coli* expression vector for the N-terminus of TIMP-4 with residues 129–195 deleted (N-TIMP-4) was generated by PCR using the mutagenic oligonucleotides 1 and 2 (Table 1), thereby introducing an *Nde*I site preceding Cys^1 and a stop codon following Gly^{128}, flanked by a unique *Eco*RI site. The PCR product was ligated into pRSET A. Ligating the *Xcm*I to *Eco*RI C-terminal domain fragment into N-TIMP-4 pRSET A generated a full-length TIMP-4 expression vector. The TIMP mutants used in this study are shown schematically in Figure 1 (top panel), and were created using the oligonucleotides summarized in Table 1 by the following procedures. The TIMP-4:TIMP-2 tail mutants were generated by cleaving the full-length TIMP-4 pRSET A construct with *Pst*I and *Hin*dIII, followed by the ligation of annealed oligonucleotides (Table 1, oligonucleotide nos. 6–11). The N-TIMP-4:C-TIMP-2 (TIMP-4 residues 1–128:TIMP-2 residues 128–194) chimaeric TIMP expression vector was generated by PCR using coding mutagenic primer no. 5 (Table 1) and a non-coding vector primer and the human TIMP-2 cDNA in pET23d as the template. The PCR product was subcloned into the *Xcm*I- and *Eco*RI-cleaved N-TIMP-4 pRSET A construct. A chimaeric TIMP N-TIMP-2:C-TIMP-4 (TIMP-2 residues 1–127:TIMP-4 residues 129–195) was constructed by PCR overlap-extension mutagenesis using vector and mutagenic primers 3 and 4. The resulting PCR product was cleaved with *Bam*HI and *Eco*RI and ligated into the N-TIMP-2 (N-terminus of TIMP-2 with residues 128–194 deleted) pET23d expression vector cleaved with these restriction enzymes. An IQ-TIMP-2 mutant (TIMP-2 with tail-sequence residues I^{192}–Q^{193} from TIMP-4) was generated by PCR, thereby replacing the E^{192}–D^{193} sequence motif of TIMP-2 with the corresponding residues in TIMP-4 using reverse mutagenic primer no. 12 (Table 1) and a coding primer upstream of the internal *Bam*HI site within the human TIMP-2 cDNA. The resulting PCR product was cleaved with *Bam*HI and *Hin*dIII and ligated into the N-TIMP-2 pET23d expression vector cleaved with these restriction enzymes.

All resulting vectors were sequenced using the dideoxy method. With the exception of N-TIMP-2:C-TIMP-4 all mutants showed the desired cDNA sequence. The N-TIMP-2:C-TIMP-4 had an additional mutation converting Lys^{116} into Arg. Lys^{116} does not interact with the target enzyme, as revealed by the X-ray structures of the MT1-MMP–TIMP-2 complex, thus allowing us to use the inhibitor in this study. *E. coli* BL21(DE3)pLysS were used to produce the seven TIMP-4 mutants. Subsequently, proteins were refolded as described for N-TIMP-2 and purified using SP-Sepharose [25].

Analysis of the structural integrity of the refolded inhibitors

The refolding of N-TIMP-4, full-length TIMP-4 and all TIMP-4 mutants was optimized using the refolding method developed previously for N-TIMP-2 [26]. The molecular masses determined under reducing conditions were 16 000 Da for N-TIMP-4 and 27 000 Da for full-length wild-type and mutant TIMP-4, while under non-reducing conditions they were found to be 14 500 and 23 000 Da (results not shown). The unfolding transition of N-TIMP-4 was highly co-operative, showing a sharp transition curve with a midpoint of denaturation at 2.35 M guanidinium chloride, a value very similar to that of N-TIMP-2 [27]. The unfolding of native TIMP-2 and refolded chimaeric or TIMP-4 tail mutants showed co-operativity with parallel shallower transition curves

© 2003 Biochemical Society

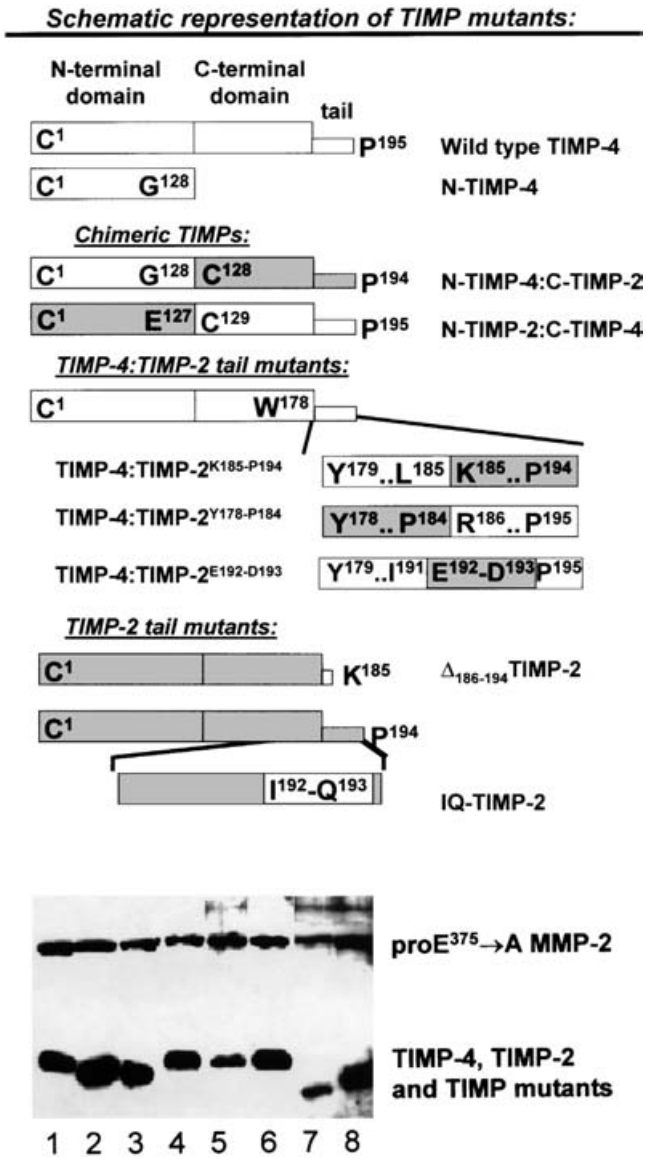

Figure 1 Schematic representation of TIMP mutants (top panel) and bimolecular complex formation between proE^{375} → A MMP-2 and wild-type and mutant TIMPs (bottom panel)

Top panel: chimaeric forms of the N- and C- domains of TIMP-2 and TIMP-4 and of TIMP-4 with portions of the TIMP-2 C-terminal 'tail' were prepared as described in the Experimental section. Sequence motifs from human TIMP-2 are represented in grey, while TIMP-4 sequence motifs are depicted in white. Amino acid residues representing domain borders are indicated. Mutants are described in the text. Bottom panel: bimolecular complexes between proE^{375} → A MMP-2 and TIMPs were generated by incubation of equimolar amounts of the purified components for 24 h, prior to isolation using gelatin–Sepharose. Bound components were detected by Western blotting using a mixture of polyclonal antibodies to TIMP-2 and TIMP-4 (lower panel) to detect bound TIMPs and a polyclonal proMMP-2 antibody to detect proE^{375} → A MMP-2 (upper panel). Lane 1, TIMP-4; lane 2, N-TIMP-2:C-TIMP-4; lane 3, N-TIMP-4:C-TIMP-2; lane 4, TIMP-4:TIMP-2$^{K185-P194}$; lane 5, TIMP-4:TIMP-2$^{Y178-P184}$; lane 6, TIMP-4:TIMP-2$^{E192-D193}$; lane 7, $\Delta_{186-194}$TIMP-2; lane 8, TIMP-2.

at lower guanidinium chloride concentrations [27]. The curves observed for the different TIMP-4 mutants showed only minor differences, indicating structural integrity and correct folding. The structural integrity of the TIMP-4 mutants was upheld by their ability to inhibit active catMT1-MMP (haemopexin domain deletion mutant of MT1-MMP with residues 269–559 deleted) and by bimolecular complex formation with proMMP-2 as shown in the Results section indicating that both the N- and C-terminal domains were correctly folded and fully functional.

Generation of TIMP-2, TIMP-4 and TIMP mutant mammalian expression vectors

Wild-type TIMP-2 in pEE12 was described previously [24]. I^{192}-Q^{193} TIMP-2 was prepared using the human TIMP-2 cDNA in pSP65 in conjunction with a reverse mutagenic primer (Table 1, oligonucleotide no. 12) encoding the IQ-TIMP-2 and a forward primer complementary to the signal sequence, which introduced a 5′ *Eco*RI site. The resulting PCR product was cleaved with *Eco*RI and *Hin*dIII and ligated into pcDNA3.1 (−). The *Bam*HI–*Hin*dIII TIMP-4 cDNA fragment was cloned into *Bam*HI- and *Hin*dIII-cleaved pcDNA3.1 (−). The N-TIMP-4:C-TIMP-2 pcDNA3.1 vector was prepared by excision of the *Xcm*I–*Hin*dIII TIMP-4 C-domain fragment and subsequent ligation of the *Xcm*I–*Hin*dIII TIMP-2 C-domain fragment from the N-TIMP-4:C-TIMP-2 pRSET A vector described above. Expression was analysed following transient transfection into COS 7 cells and confirmed that the vectors were fully functional (results not shown).

Characterization of a polyclonal antibody against N-TIMP-4

HPLC purified N-TIMP-4 was used to produce a polyclonal antiserum in sheep [28]. The antibody was affinity purified using TIMP-4 and shown to react specifically with N-TIMP-4, TIMP-4 and N-TIMP-4:C-TIMP-2 by Western blotting, but it did not cross-react with other TIMPs (results not shown).

Recombinant MMPs

Recombinant wild-type and mutant proMMP-2 were produced using stably transfected mouse myeloma cells and purified from the cell-conditioned medium (Figure 2, top panel) [29,30]. A soluble form of MT1-MMP comprised of the propeptide and the catalytic domain, pro-catMT1-MMP, was expressed in BL21(DE3)pLysS using a pRSET B construct, refolded from inclusion bodies and purifed by Ni^{2+}-nitrilotriacetate–agarose chromatography. The purified refolded protein was dialysed to remove imidazole, which resulted in partial spontaneous activation. Full activation was achieved by incubation for 15 min at 37 °C, which resulted in spontaneous conversion to the fully processed form of the enzyme [25,31].

Bimolecular complexes between proMMP-2 mutants and TIMP-4 mutants

Wild proMMP-2, C-terminal-deleted pro$\Delta_{418-631}$MMP-2 and C-terminal domain stromelysin-1 (SL) chimaeras of proMMP-2 (Figure 2, top panel) [32] were incubated with 2-fold molar excess of either wild-type or mutant TIMP-4 for 24 h in order to allow complex formation. The complexes were isolated using gelatin–Sepharose.

Analysis of trimolecular complex formation between active catMT1-MMP, wild-type and mutant TIMP-4 and E^{375} → A inactive point mutant of proMMP-2 (proE^{375} → A MMP-2)

Bimolecular complexes between proE^{375} → A MMP-2 and mutant TIMPs were incubated with a 2-fold molar excess of active catMT1-MMP to allow trimolecular complex formation. Similar

© 2003 Biochemical Society

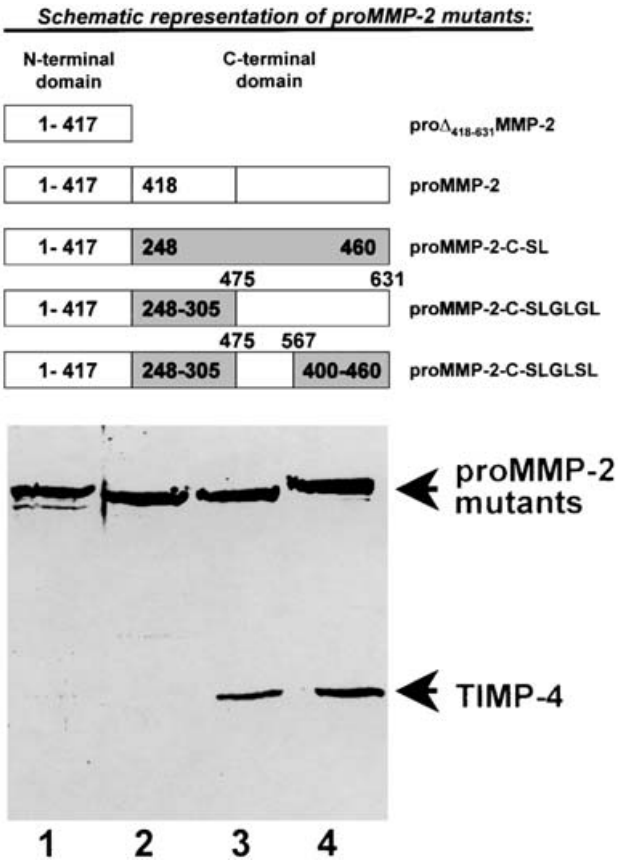

Figure 2 Schematic representation of proMMP-2 mutants (top panel) and bimolecular complex formation between TIMP-4 and proMMP-2 C-terminal domain mutants (bottom panel)

Top panel: the MMP-2 C-terminal haemopexin domain was replaced by portions of SL C-terminal domain as detailed in [29]. SL domains are represented in grey and the corresponding amino acid residues of SL are indicated. The bordering amino acid residues from MMP-2 (GL) are indicated on the left of the diagram. Mutants are described in the text. Bottom panel: the MMP-2 and MMP-3 C-terminal domain chimaeric proteins described in the top panel were incubated with TIMP-4 and the complexes isolated by gelatin-affinity chromatography. The formation of bimolecular complexes was established by the presence of TIMP-4 in the matrix eluates prepared as described in the Experimental section and analysed by SDS/PAGE. Lane 1, proMMP-2-C-SL; lane 2, proMMP-2-C-SLGLSL; lane 3, proMMP-2-C-SLGLGL; lane 4, wild-type proMMP-2. The protein band corresponding to TIMP-4 is indicated on the right. The gel was processed under reducing conditions.

experiments were performed with a bimolecular complex between proE^{375} → A MMP-2 and TIMP-2 (proE^{375} → A MMP-2–TIMP-2) as a positive control for trimolecular complex formation. The respective trimolecular complexes were isolated using gelatin–Sepharose chromatography.

Kinetic analysis of enzyme inhibitor interactions

The concentrations of the active enzymes were estimated by titration against TIMP-1 or TIMP-2 of known concentration, as appropriate [33]. The concentration of TIMP-4 and N-TIMP-4 were determined using MMP-13 of known concentration. The kinetics for the inhibition of active catMT1-MMP and active MMP-2 with wild-type and N-TIMP-4 were analysed by evaluation of the second-order rate constant k_{on} [23]. The apparent K_i^{app} values for inhibition of catMT1-MMP were determined following a 24 h preincubation period at 25 °C to establish equilibrium [25]. The apparent K_i^{app} values for inhibition of MMP-2 could not be determined due to their low values [34]. All reactions were performed with McaPLGLDpaARNH$_2$ [7-methoxycoumarin-(4-yl)acetyl-Pro-Leu-Gly-Leu-*N*-3(2,4-dinitrophenyl)-L-2,3-diaminopropionyl-Ala-Arg] as the substrate at 25 °C using a PerkinElmer spectrofluorimeter (LS 50B) [35].

SDS/PAGE and Western Blotting

Samples to be analysed by SDS/PAGE were diluted 1:1 with SDS sample buffer (100 mM Tris/HCl, pH 6.8/10 % SDS/10 % glycerol with or without 1 % β-mercaptoethanol) and boiled for 5 min prior to SDS/PAGE using 12 % or 10 % acrylamide separation gels and staining with Coomassie Brilliant Blue. Western blots were developed using polyclonal antibodies to MT1-MMP [32], proMMP-2 and TIMP-4 (J. R. Worley, R. M. Hembry and V. Knäuper, unpublished work) and a peroxidase-conjugated donkey anti-sheep antibody (Jackson Immunoresearch) and visualized by ECL.

Cellular activation of proMMP-2 by MT1-MMP in *TIMP-2*$^{-/-}$ cells

Immortalized fibroblasts from *TIMP-2*$^{-/-}$ mice were transfected with *Pvu*I-linearized MT1-MMP cDNA in pcDNA3.1 zeo (+) and stable cell lines were established following selection with 250 μg/ml zeocin. Cells (15×10^4) were seeded on to 12-well plates and transiently transfected with expression vectors for TIMP-2 (in pEE12), IQ-TIMP-2 [in pcDNA3.1 (−)] or wild-type and mutant TIMP-4 [in pcDNA3.1 (−)] using Fugene transfection reagent (Invitrogen), and supplemented with 100 ng/ml proMMP-2 in serum-free medium. Alternatively, 30×10^4 cells were seeded on to 12-well plates and serum-free medium supplemented with increasing amounts of either wild-type TIMP-4 or TIMP-2 and 100 ng/ml recombinant proMMP-2. After 24 or 48 h the cell-conditioned medium and lysates were analysed for the presence of active MMP-2. Processing of MT1-MMP was analysed by Western blot analysis using a polyclonal antibody to MT1-MMP [32].

MT1-MMP-containing membranes

TIMP-2$^{-/-}$ mouse fibroblasts transfected with MT1-MMP were grown in the presence of 1 μM of the MMP inhibitor BB94, to stabilize cell-surface MT1-MMP. When 80 % confluent, the cells were washed three times with Dulbecco's modified Eagle's medium, pH 9.0, which results in rapid dissociation of BB94 from the MT1-MMP at this high pH. Cells were scraped from the flasks and pelleted by centrifugation (1200 ***g***). Lysates were prepared by resuspending cells in 5 mM Tris/HCl (pH 7.6), 100 μM PMSF, 1 μg/ml pepstatin A and 1 μg/ml E-64 [*trans*-epoxysuccinyl-L-leucylamido-(4-guanidino)butane], and incubated on ice before homogenization through a narrow-gauge needle (26 G). Membranes were isolated by the method described previously [36].

RESULTS

TIMP-2 and TIMP-4 share some important features, such as the ability to form bimolecular complexes with proMMP-2 [13], yet they show profound differences in their ability to facilitate proMMP-2 activation by MT1-MMP at the cell surface [14,16]. In order to advance our knowledge of the domain and sequence requirements of TIMP-2 allowing activation of proMMP-2 by MT1-MMP we introduced domains and sequence motifs of TIMP-4 into TIMP-2 and determined their effect on bimolecular

© 2003 Biochemical Society

complex formation with proMMP-2, their ability to establish trimolecular complexes with proE^{375} → A MMP-2 and catMT1-MMP and their ability to facilitate proMMP-2 activation by MT1-MMP in a *TIMP-2*$^{-/-}$ cellular model system.

Bimolecular complex formation: domain requirements of proMMP-2 for TIMP-4

Initially we investigated whether TIMP-4 interacts with proMMP-2 in a similar way to TIMP-2 to establish the proMMP-2 domain requirements in this process. In an earlier study we found that TIMP-2 bound to proMMP-2 via the haemopexin domain and was a weaker inhibitor of MMP-3, due to a lack of C-domain interactions [29], even though these domains share 50% homology. The same chimaeric proteins comprised of the N- and C-domains of MMP-2 and SL were used as in Butler et al. [29] (Figure 2, top panel) to identify the proMMP-2 sequences that TIMP-4 binds to. Purified wild-type proMMP-2 and chimaeric forms of proMMP-2 with the C-domain of SL were incubated with TIMP-4 and N-TIMP-4. The complexes were isolated by affinity chromatography using gelatin–Sepharose followed by analysis of components present using SDS/PAGE (Figure 2, bottom panel). The C-terminal deletion mutant of proMMP-2 (pro$\Delta_{418-631}$MMP-2) did not bind to either N-TIMP-4 or wild-type TIMP-4 (results not shown), indicating that the C-terminal domain of the enzyme was essential for proenzyme binding. In contrast, wild-type proMMP-2 and proMMP-2-C-SLGLGL (proMMP-2 mutant encoding C-terminal domain residues 248–305 from SL and residues 475–631 from MMP-2) formed a complex with wild-type TIMP-4 (Figure 2, bottom panel), while proMMP-2-C-SL (proMMP-2 mutant encoding the C-terminal domain of SL residues 248–460) and proMMP-2-C-SLGLSL (proMMP-2 mutant encoding C-terminal domain residues 248–305 and 400–460 from SL and residues 475–567 from MMP-2) showed no binding. N-TIMP-4 did not bind to either wild-type proMMP-2 or any of the proMMP-2 mutants, thereby underlining the dependence of proenzyme complex formation on C-terminal inhibitor interactions (results not shown). The binding motif for TIMP-4 was therefore localized in blades 3 and 4 of the β-propeller of proMMP-2 complementary to the TIMP-2-binding site, shown previously to be essential for activation of proMMP-2 by MT1-MMP [29]. Since TIMP-4 does not potentiate proMMP-2 activation by MT1-MMP [37] these C-terminal domain interactions must be considerably weaker, which was confirmed by kinetic analysis of the association rate constant k_{on} for active MMP-2, which was 1.6×10^6 M^{-1} s^{-1}, and thus 3.6 times lower than that for TIMP-2 (5.9×10^6 M^{-1} s^{-1}). Our data are in a similar range to previously published data by Bigg et al. [14].

Characterization of the structural integrity of the C-terminal domains of TIMP-2 and TIMP-4 mutants: bimolecular complex formation with proE^{375} → A MMP-2

In order to establish that the TIMP mutants (Figure 1, top panel) had a correctly folded C-terminal domain we assessed their ability to establish bimolecular complexes with the inactive proMMP-2 mutant proE^{375} → A MMP-2. All mutants were incubated with equimolar concentrations of proE^{375} → A MMP-2 for 24 h at room temperature. The reaction mixtures were then applied to gelatin–Sepharose matrices and bound proteins were eluted with 10% DMSO in buffer. The eluted proteins were analysed by Western blotting to determine which TIMPs were able to form a bimolecular complex with proE^{375} → A MMP-2. With the exception of N-TIMP-4 and N-TIMP-2 (results not shown), all other TIMP mutants were detected by Western blotting in the gelatin-bound phase (Figure 1, bottom panel). Therefore, like TIMP-2, TIMP-4 and the mutated TIMPs were capable of forming a bimolecular complex with proE^{375} → A MMP-2, indicating the structural integrity of their C-terminal domain.

Table 2 Kinetic parameters for the inhibition of active catMT1-MMP by N-TIMP-4, TIMP-4 and the proE^{375} → A MMP-2–TIMP-4 complex

Measurements were performed at 112 or 25 pM enzyme concentration and a constant temperature of 25 °C using 1 μM McaPLGLDpaARNH$_2$ [7-methoxycoumarin-(4-yl)acetyl-Pro-Leu-Gly-Leu-*N*-3(2,4-dinitrophenyl)-L-2,3-diaminopropionyl-Ala-Arg] as the substrate.

Inhibitor	Apparent K_i (pM)	K_{on} (M^{-1} · s^{-1})
N-TIMP-4	834 ± 98	9.5×10^4
TIMP-4	< 2.6 ± 1.3	3.9×10^5
proE^{375} → A MMP-2–TIMP-4	< 3.2 ± 1.5	2.3×10^5

Inhibition of active catMT1-MMP by N-TIMP-4, TIMP-4 and the proE^{375} → A MMP-2–TIMP-4 complex

The apparent K_i and k_{on} values for catMT1-MMP and N-TIMP-4, full-length TIMP-4 and the proE^{375} → A MMP-2–TIMP-4 complex were measured (Table 2). These experiments were designed to determine the effect of the inhibitor C-terminal domain on the association rate of enzyme inhibitor complex formation (k_{on}) and overall stability of the complexes (K_i). Additionally, the effect of bound proE^{375} → A MMP-2 to TIMP-4 was assessed to establish whether C-terminally bound proE^{375} → A MMP-2 would influence the k_{on} and apparent K_i with active catMT1-MMP.

The k_{on} values for catMT1-MMP binding to TIMP-4 and the proE^{375} → A MMP-2–TIMP-4 complex were found to be in the range of $(1–4) \times 10^5$ M^{-1} · s^{-1}. Since the association rate for the proE^{375} → A MMP-2–TIMP-4 complex, full-length TIMP-4 and N-TIMP-4 and catMT1-MMP were of the same order of magnitude we can conclude that the C-terminal domain plays no role in catMT1-MMP inhibitor association.

The apparent K_i values for inhibition of catMT1-MMP with full-length TIMP-4 and proE^{375} → A MMP-2–TIMP-4 complex were found to be in the range ≈2.6 to ≈3.2 pM. In contrast, the apparent K_i value for N-TIMP-4 and catMT1-MMP was 834 pM, a 300-fold increase when compared with full-length TIMP-4 or the proE^{375} → A MMP-2–TIMP-4 complex. The catMT1-MMP complex with N-TIMP-4 was less stable due to lack of C-terminal domain interactions. Thus our data show for the first time that the affinity for the interaction between catMT1-MMP and full-length TIMP-4 is dependent on C-domain interactions with the catalytic domain of a target MMP. This contrasts with TIMP-2 interactions with catMT1-MMP, where the C-domain of TIMP-2 appears to show negligible binding to the enzyme [29].

Characterization of a cellular model system for proMMP-2 activation using *TIMP-2*$^{-/-}$ cells

Analysis of MT1-MMP expression and auto proteolysis of MT1-MMP in *TIMP-2*$^{-/-}$ cells

A cellular model system for proMMP-2 activation by MT1-MMP was established by transfection of immortalized fibroblasts from *TIMP-2*$^{-/-}$ mice with a pcDNA3.1 vector encoding MT1-MMP. Western blot of cell lysates showed that MT1-MMP-transfected cells expressed human proMT1-MMP (molecular

© 2003 Biochemical Society

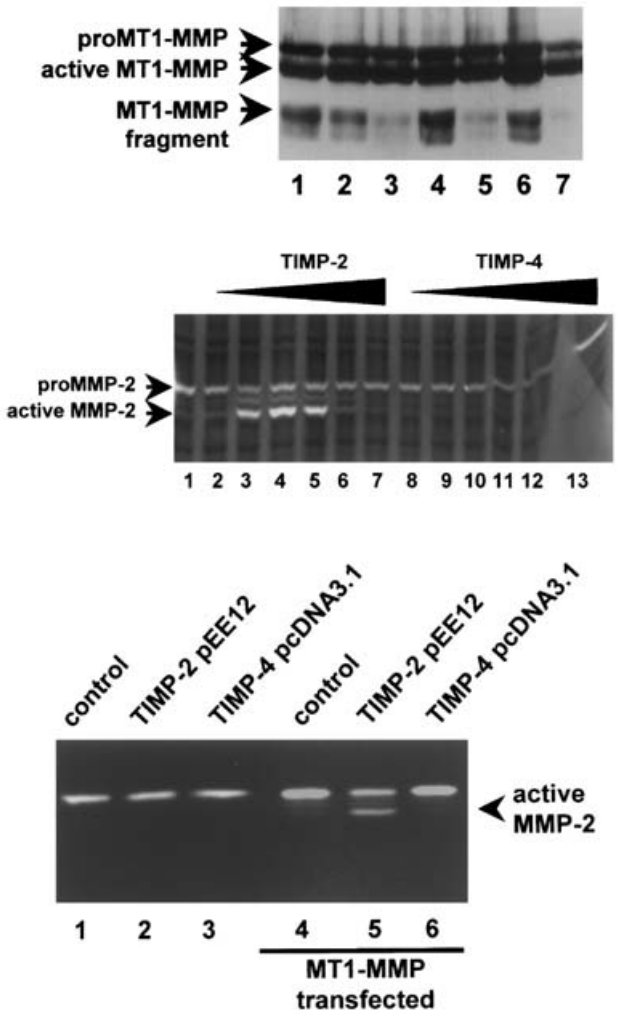

Figure 3 Inhibition of MT1-MMP fragmentation (top panel) and activation of proMMP-2 by MT1-MMP in *TIMP-2*$^{-/-}$ cells: effects of exogenous TIMPs (middle panel) and co-expression of TIMP-2 and TIMP-4 (bottom panel)

Top panel: *TIMP-2*$^{-/-}$ cells expressing MT1-MMP were incubated with 5 and 100 nM TIMP-2, TIMP-4 and the proE^{375} → A MMP-2–TIMP-4 complex for 24 h followed by the analysis of the cell lysates by Western blotting for the presence of pro- and active MT1-MMP and the inactive 44000 Da MT1-MMP fragment. Lane 1, no inhibitor; lanes 2 and 3, 5 and 100 nM TIMP-2; lanes 4 and 5, 5 and 100 nM TIMP-4; lanes 6 and 7, 5 and 100 nM proE^{375} → A MMP-2–TIMP-4 complex. Specific staining for active MT1-MMP, and the 44000 Da MT1-MMP fragment, is indicated on the left. Middle panel: effect of exogenous TIMPs. Cells were incubated with various amounts of TIMP-2 or TIMP-4 and proMMP-2 (1 μg/ml) for 48 h. Analysis of cell lysates for active MMP-2 was carried out using gelatin zymography. Lane 1, proMMP-2 incubated for 48 h with MT1-MMP-overexpressing *TIMP-2*$^{-/-}$ fibroblasts; lanes 2–7, as lane 1 with increasing amounts of human TIMP-2; lanes 8–13, as lane 1 with increasing amounts of TIMP-4: 0.1 nM, lanes 2 and 8; 1 nM, lanes 3 and 9; 5 nM, lanes 4 and 10; 10 nM, lanes 5 and 11; 20 nM, lanes 6 and 12; 40 nM, lanes 7 and 13. Active MMP-2 is indicated on the left. Bottom panel: effect of co-expression of TIMP-2 and TIMP-4. *TIMP-2*$^{-/-}$ cells (lanes 1–3) and MT1-MMP-transfected *TIMP-2*$^{-/-}$ cells (lanes 4–6) were incubated for 24 h with proMMP-2, and were untransfected (lanes 1 and 4), transiently transfected with TIMP-2 (lanes 2 and 5) or transiently transfected with TIMP-4 (lanes 3 and 6).The cell-conditioned medium was analysed by gelatin zymography. Active MMP-2 is indicated on the right.

mass 63 000 Da), active MT1-MMP (60 000 Da) and the inactive C-terminal domain fragment (44 000 Da) that is still associated with the membrane (Figure 3, top panel, lane 1). Exogenous addition of either TIMP-4, the proE^{375} → A MMP-2–TIMP-4 complex or TIMP-2 showed that fragmentation of MT1-MMP was strongly inhibited (Figure 3, top panel, lanes 3, 5 and 7). We concluded that degradation of MT1-MMP to the inactive fragment is dependent on MT1-MMP activity and is therefore autoproteolytic, as this was efficiently inhibited by TIMP-2, TIMP-4 and the proE^{375} → A MMP-2–TIMP-4 complex. Furthermore our cells did not produce detectable amounts of proMMP-2; however, we cannot exclude that other MMPs may contribute to MT1-MMP fragmentation.

Analysis of proMMP-2 activation in the presence and absence of TIMPs by MT1-MMP-transfected *TIMP-2*$^{-/-}$ cells

Gelatin zymography of cell lysates from MT1-MMP-transfected *TIMP-2*$^{-/-}$ fibroblasts show that activation of proMMP-2 was impaired in the absence of TIMP-2 (Figure 3, middle panel, lane 1), and was restored with 1–10 nM TIMP-2, showing reappearance of active MMP-2 in the cell lysate (Figure 3, middle panel, lanes 3–5). Cellular activation of proMMP-2 in the presence of full-length TIMP-4 was then compared with TIMP-2 and showed that TIMP-4 was unable to promote activation under our experimental conditions (Figure 3, middle panel, lanes 8–13).

To confirm further that TIMP-4 was unable to promote proMMP-2 activation by cell-associated MT1-MMP we transiently transfected *TIMP-2*$^{-/-}$ fibroblasts and MT1-MMP-expressing *TIMP-2*$^{-/-}$ fibroblasts with expression vectors for TIMP-2 or TIMP-4. Activation of proMMP-2 was observed with MT1-MMP-expressing cells transiently transfected with pEE12 TIMP-2, releasing the active form into the conditioned medium (Figure 3, bottom panel, lane 5), but no activation of proMMP-2 was observed with cells that did not express MT1-MMP (Figure 3, bottom panel, lane 2). Transient transfection of both cell types with the pcDNA 3.1(−) TIMP-4 only revealed proMMP-2 in the cell-conditioned medium (Figure 3, bottom panel, lanes 3 and 6). Thus both approaches demonstrated that TIMP-4 was unable to potentiate proMMP-2 activation by MT1-MMP, which is in agreement with previously published work [14]. Thus this cellular model system allowed us to use our TIMP-4 mutants to analyse gain of activating function in the MT1-MMP-transfected *TIMP-2*$^{-/-}$ cells.

The role of the N- and C-terminal domains of TIMP-2 in trimolecular complex formation with proE^{375} → A MMP-2 and active catMT1-MMP

To be able to define the sequence requirements for TIMP-2-dependent activation of proMMP-2 by MT1-MMP, we introduced TIMP-2 domains and sequence motifs into the related inhibitor, TIMP-4 (see Figure 1, top panel, for details) [15,38]. Bimolecular complexes between wild-type TIMP-2, TIMP-4 and the chimaeric inhibitors N-TIMP-2:C-TIMP-4 and N-TIMP-4:C-TIMP-2 were generated by incubating the inhibitors with proE^{375} → A MMP-2 and isolated following gelatin–Sepharose chromatography. These bimolecular complexes were then incubated with active catMT1-MMP for 24 h at room temperature to allow the formation of possible trimolecular complexes. The mixtures were applied to gelatin–Sepharose matrices and bound proteins were analysed by Western blotting for the presence of catMT1-MMP forming a complex with wild-type or mutant TIMPs and proE^{375} → A MMP-2. As shown in Figure 4 (top panel) only TIMP-2 and the chimaeric inhibitor N-TIMP-4:C-TIMP-2 supported binding of active catMT1-MMP to the respective proE^{375} → A MMP-2–TIMP complex, thereby identifying the C-terminal domain of TIMP-2 as the determinant for trimolecular complex formation between proE^{375} → A MMP-2, TIMP-2 and catMT1-MMP. Our data also show that the proE^{375} → A MMP-2–TIMP-4 and proE^{375} → A MMP-2–N-TIMP-2:C-TIMP-4 complexes dissociated when active catMT1-MMP was present. These

© 2003 Biochemical Society

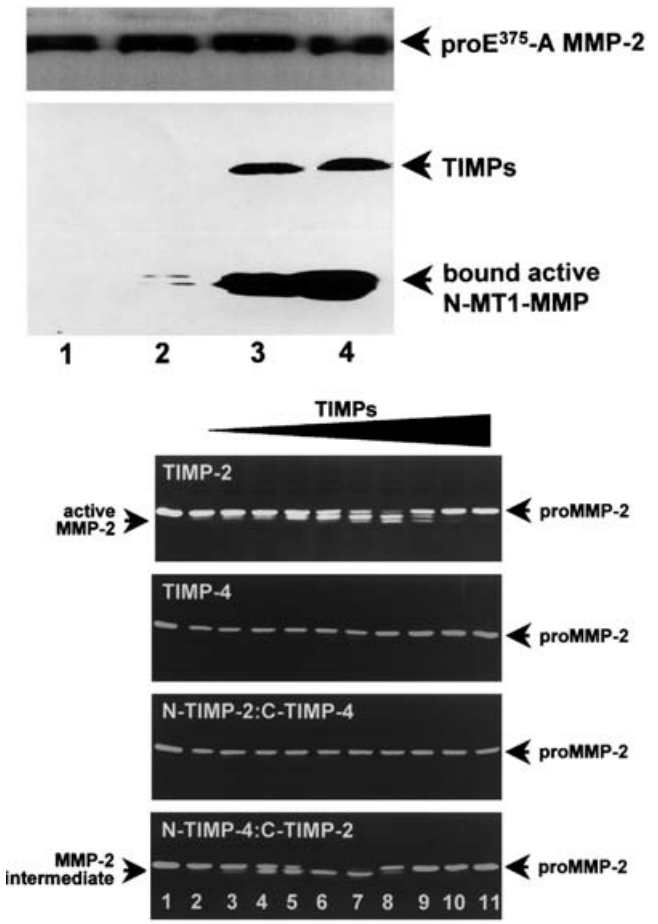

Figure 4 Trimolecular complex formation and dependency on the C-terminal domain of *TIMP-2* (top panel) and reconstitution of proMMP-2 activation by MT1-MMP under TIMP-2-free conditions by N-TIMP-4:C-TIMP-2 (bottom panel)

Top panel: bimolecular complexes between wild-type and mutant TIMP-4 and proE^{375} → A MMP-2 were incubated with a 2-fold molar excess of active catMT1-MMP for 24 h at room temperature, to allow trimolecular complex formation. Complexes were isolated using gelatin–Sepharose and the bound proteins were detected by Western blot analysis using a mixture of antibodies to proMMP-2 (top), TIMP-4 and human TIMP-2 (middle) and active catMT1-MMP (bottom) as indicated on the right. Lane 1, TIMP-4; lane 2, N-TIMP-2:C-TIMP-4; lane 3, N-TIMP-4:C-TIMP-2; lane 4, TIMP-2. Please note the lack of signal for TIMP-4 and N-TIMP-2:C-TIMP-4 in the middle panel, which is due to complex dissociation from proE^{375} → A MMP-2 and complex formation with active catMT1-MMP, which does not bind to gelatin–Sepharose. Bottom panel: MT1-MMP-containing membranes from our transfected *TIMP-2*$^{-/-}$ cells were incubated for 24 h at 37 °C with varying concentrations of TIMP-2, TIMP-4, N-TIMP-2:C-TIMP-4 and N-TIMP-4:C-TIMP-2 in the presence of proMMP-2 (1 μg/ml). Processing of proMMP-2 was monitored by zymography. All zymogramms were loaded identically. Lane 1, proMMP-2 buffer control; lane 2, proMMP-2 with membranes; lanes 3–11, as lane 2 but incubated in the presence of increasing amounts of TIMPs: 0.01 nM, lane 3; 0.05 nM, lane 4; 0.1 nM, lane 5; 0.5 nM, lane 6; 1 nM, lane 7; 2.5 nM, lane 8; 5 nM, lane 9; 10 nM, lane 10; 20 nM, lane 11.

experiments were performed with an excess of catMT1-MMP and thus the Western blots show loss of signal for TIMP-4 and N-TIMP-2:C-TIMP-4 (Figure 4, top panel, TIMPs, lanes 1 and 2).

The role of the N- and C-terminal domains of TIMP-2 in proMMP-2 activation by MT1-MMP in *TIMP-2*$^{-/-}$ cells

To establish whether the ability of a TIMP to allow trimolecular complex formation with catMT1-MMP and proMMP-2 would be an important determinant for proMMP-2 activation at the cell surface we performed additional cellular-activation experiments using our MT1-MMP-expressing *TIMP-2*$^{-/-}$ cells or membranes isolated from these cells. Initially, cells were seeded into six-well culture dishes and serum-free medium was supplemented with proMMP-2 and N-TIMP-2:C-TIMP-4 or N-TIMP-4:C-TIMP-2. Analyses of proMMP-2 processing by zymography showed that the intermediate form was generated in the presence of N-TIMP-4:C-TIMP-2, whereas N-TIMP-2:C-TIMP-4 was completely inactive (results not shown). This observation was confirmed using MT1-MMP-containing membranes from *TIMP-2*$^{-/-}$ cells, which were incubated in the presence of the mutant TIMPs and proMMP-2. TIMP-2 allowed processing of proMMP-2 to the fully active form, while TIMP-4 and N-TIMP-2:C-TIMP-4 were unable to support any processing of proMMP-2 (Figure 4, bottom panel, compare panels for TIMP-2, TIMP-4 and N-TIMP-2:C-TIMP-4). In contrast, N-TIMP-4:C-TIMP-2 showed proMMP-2 activation capability; however, the intermediate form of MMP-2 was again generated (Figure 4, bottom panel, N-TIMP-4:C-TIMP-2), with minute amounts of active form detectable. This suggested that N-TIMP-4:C-TIMP-2 was impaired to support conversion into the fully active enzyme but could efficiently mediate activation to the intermediate form, which is the cleavage event that depends on MT1-MMP activity [19].

To establish why N-TIMP-4:C-TIMP-2 was only capable of promoting processing of proMMP-2 to the intermediate form we determined the association rate constant k_{on} for the binding of mutant TIMPs to MMP-2. Strikingly N-TIMP-4:C-TIMP-2 as well as N-TIMP-2:C-TIMP-4 (0.48×10^6 $M^{-1} \cdot s^{-1}$) showed a dramatic reduction in their association rate constant k_{on} by an order of magnitude, when compared with wild-type TIMP-2 (5.9×10^6 $M^{-1} \cdot s^{-1}$), which could explain the observed conversion into the intermediate form of MMP-2.

The role of the TIMP-2 tail-sequence motifs in trimolecular complex formation with proE^{375} → A MMP-2 and active catMT1-MMP: analysis of the TIMP-4:TIMP-2 tail mutants

The TIMP-2 tail-deletion mutant ($\Delta_{186-194}$TIMP-2; TIMP-2 with residues 186–194 deleted) failed to establish a stable trimolecular complex with proE^{375} → A MMP-2 and catMT1-MMP (results not shown), although this inhibitor was still able to form a bimolecular complex with proE^{375} → A MMP-2 (Figure 1, bottom panel). This suggested that residues in the tail sequence of TIMP-2 are involved in trimolecular complex formation. To determine whether the TIMP-4 tail-sequence motif was responsible for failure of the inhibitor to establish a stable trimolecular complex with proE^{375} → A MMP-2 and catMT1-MMP we replaced this sequence motif with parts of the TIMP-2 tail sequence (for details see Figure 1, top panel). TIMP-4:TIMP-2$^{K185-P194}$, which carries the 10 C-terminal amino acid residues (185–194) of TIMP-2, was able to support trimolecular complex formation (Figure 5, top panel, lane 1). The amount of catMT1-MMP bound was markedly reduced when compared with N-TIMP-4:C-TIMP-2 or TIMP-2 (Figure 4, top panel, lanes 3 and 4), which indicated that the three C-terminal loops, derived from TIMP-2, contributed to some degree to trimolecular complex formation, but were not the sole determinants in this process. However, the tail mutant TIMP-4:TIMP-2$^{Y178-P184}$ (TIMP-4 with tail-sequence residues 178–184 from TIMP-2) was unable to support a trimolecular complex (Figure 5, top panel, lane 2) and confirmed our data using the tail-deletion mutant $\Delta_{186-194}$TIMP-2 that lacked the same sequence motif, ^{187}EFLDIEDP^{194}. These results indicated that the last 10 amino acid residues in TIMP-2 are vital for stable trimolecular

© 2003 Biochemical Society

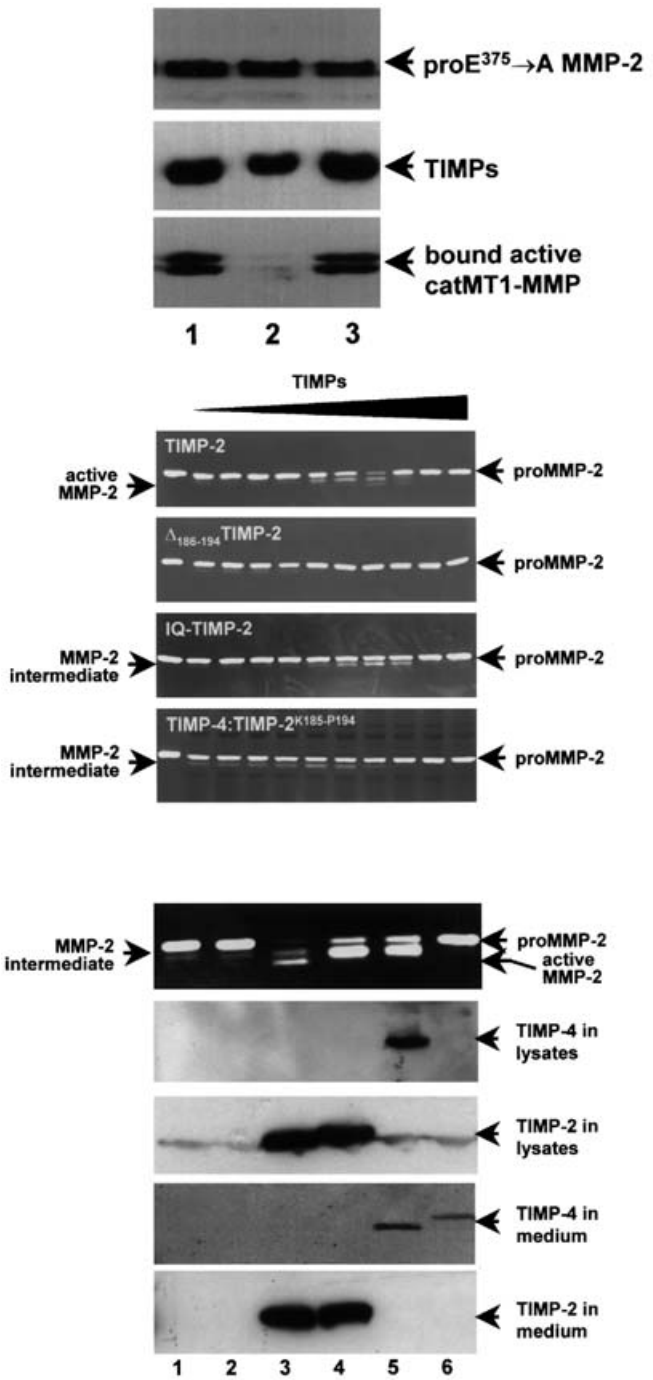

Figure 5 Trimolecular complex formation and dependency on the charged tail of TIMP-2 (top panel), reconstitution of proMMP-2 activation by (middle panel) MT1-MMP-containing membranes; dependency on the charged tail of TIMP-2 and (bottom panel) MT1-MMP-overexpressing cells from the *TIMP-2*$^{-/-}$ mice using expression vectors for various wild-type and mutant TIMPs

Top panel: bimolecular complexes between the TIMP-4:TIMP-2 tail mutants and proE^{375} → A MMP-2 were incubated with active catMT1-MMP at a 2:1 molar ratio for 24 h at room temperature, to allow trimolecular complex formation. Complexes were isolated using gelatin–Sepharose and the bound proteins were detected by Western blot analysis using antibodies to proMMP-2 (top), TIMP-4 (middle) and active catMT1-MMP (bottom) as indicated on the right. Lane 1, TIMP-4:TIMP-2$^{K185-P194}$; lane 2, TIMP-4:TIMP-2$^{Y178-P184}$; lane 3, TIMP-4:TIMP-2$^{E192-D193}$. Note that TIMP-4:TIMP-2$^{Y178-P184}$ was unable to establish a trimolecular complex with proE^{375} → A MMP-2 and active catMT1-MMP and therefore lacks a signal for active catMT1-MMP. Middle panel: lane 1, recombinant proMMP-2 (1 μg/ml) was incubated at 37 °C for 16 h with buffer; lane 2, proMMP-2 incubated with membranes prepared from *TIMP-2*$^{-/-}$ mouse fibroblasts transfected with MT1-MMP; lanes 3–11, as lane 2 but incubated with increasing amounts of TIMP-2, $\Delta_{186-194}$TIMP-2, IQ-TIMP-2 or TIMP-4:TIMP-C$^{K185-P194}$: 0.01 nM, lane 3; 0.05 nM, lane 4; 0.1 nM, lane 5; 0.5 nM, lane 6; 1 nM, lane 7; 2.5 nM, lane 8; 5 nM, lane 9; 10 nM, lane 10; 20 nM, lane 11. Bottom panel: MT1-MMP-transfected cells from the *TIMP-2*$^{-/-}$ mice were transiently transfected with mammalian expression vectors for TIMP-2, IQ-TIMP-2, N-TIMP-4:C-TIMP-2 and TIMP-4 (for details see the Experimental section) and incubated with proMMP-2 for 24 h at 37 °C. Lane 1, cells with proMMP-2; lane 2, cells with fugene and proMMP-2; lane 3, cells transfected with TIMP-2; lane 4, cells transfected with IQ-TIMP-2; lane 5, cells transfected with N-TIMP-4:C-TIMP-2; lane 6, cells transfected with TIMP-4. Note loading was identical for all parts of this Figure. First panel: analysis for proMMP-2 activation using zymography. Second panel: analysis for the presence of wild-type and mutant TIMP-4 in cell lysates by Western blotting using a TIMP-4 specific antibody. Third panel: analysis for the presence of wild-type and mutant TIMP-2 in cell lysates by Western blotting using a TIMP-2-specific antibody. Fourth panel: analysis for the presence of wild-type and mutant TIMP-4 in medium by Western blotting using a TIMP-4-specific antibody. Fifth panel: analysis for the presence of wild-type and mutant TIMP-2 in medium by Western blotting using a TIMP-2-specific antibody.

complex formation between the inhibitor and proE^{375} → A MMP-2 and catMT1-MMP.

To define further the sequence requirements for proE^{375} → A MMP-2–TIMP-2–catMT1-MMP trimolecular complex formation, the tail mutant TIMP-4:TIMP-2$^{E192-D193}$ (TIMP-4 with tail-sequence residues 192–193 from TIMP-2) was generated and analysed. The data revealed that this mutant showed binding of both proE^{375} → A MMP-2 and catMT1-MMP in a trimolecular complex with the inhibitor (Figure 5, top panel, lane 3). Thus in conclusion our data show that two amino acid residues within the tail-sequence motif of TIMP-2 contribute considerably to its ability to support stable trimolecular complex formation with proE^{375} → A MMP-2 and catMT1-MMP.

The role of the TIMP-2 tail-sequence motifs in proMMP-2 activation by MT1-MMP using *TIMP-2*$^{-/-}$ cells: analysis of the TIMP-4:TIMP-2 tail mutants

To define further the sequence requirements of TIMP-2 in proMMP-2 activation by MT1-MMP, we performed additional cell-activation experiments using the TIMP-4:TIMP-2 tail mutants. Our results showed that only small amounts (≈15%) of the MMP-2 activation intermediate were generated by the tail mutant TIMP-4:TIMP-2$^{K185-P194}$. In contrast, the tail mutants TIMP-4:TIMP-2$^{Y178-P184}$ and TIMP-4:TIMP-2$^{E192-D193}$ showed no detectable conversion into the intermediate form (results not shown). Identical results were obtained using the TIMP-2-free MT1-MMP-containing membranes (Figure 5, middle panel, TIMP-4:TIMP-2$^{K185-P194}$). This result was expected since few residues remained from TIMP-2. The TIMP-4 N-terminal domain showed reduced favourable N-terminal interactions between inhibitor and MT1-MMP. In addition, these TIMP-4:TIMP-2 tail mutants bound lower levels of catMT1-MMP when compared with N-TIMP-4:C-TIMP-2, indicating a reduced ability to form trimolecular complexes (compare Figure 4, top panel, with Figure 5, top panel, bound active catMT1-MMP). This suggested that the TIMP-4:TIMP-2 tail-mutant complexes with MT1-MMP and proE^{375} → A MMP-2 were less stable.

The role of the TIMP-2 tail sequence in proMMP-2 activation by MT1-MMP in *TIMP-2*$^{-/-}$ cells: analysis of $\Delta_{186-194}$TIMP-2 and IQ-TIMP-2

We used a TIMP-2 tail-deletion mutant, $\Delta_{186-194}$TIMP-2 [23], to investigate whether our hypothesis that the tail sequence ^{187}EFLDIEDP^{194} of TIMP-2 was involved in activation of

© 2003 Biochemical Society

proMMP-2 by MT1-MMP was correct. As shown in Figure 5 (middle panel), the tail-deletion mutant $\Delta_{186-194}$TIMP-2 was unable to promote processing of proMMP-2 by MT1-MMP-containing membranes, demonstrating loss of function.

To narrow down the sequence requirements further, we generated an additional full-length TIMP-2 mutant, designated IQ-TIMP-2 (Figure 1, top panel) to confirm our hypothesis that the tail-sequence motif E^{192}–D^{193} (converted to I^{192}–Q^{193}) is a major determinant in mediating cellular activation of proMMP-2 by MT1-MMP. The IQ-TIMP-2 was analysed using either transient transfections of the cDNA in pcDNA3.1 (–) into the MT1-MMP-expressing cells from the *TIMP-2*$^{-/-}$ mice or by performing membrane-activation experiments using the purified inhibitor followed by analysis of proMMP-2 activation. The analysis of the respective zymogram revealed that proMMP-2 was converted into the intermediate form only, thus showing partial loss of activation capability (Figure 5, middle panel, IQ-TIMP-2, and Figure 5, bottom panel, zymogram, lane 4).

Kinetic analysis of the association rate constant k_{on} for IQ-TIMP-2 with MMP-2 revealed a dramatic reduction in the association rate constant k_{on} to 0.45×10^6 $M^{-1} \cdot s^{-1}$. This was an order of magnitude lower than the wild type, similar to the value determined for N-TIMP-4:C-TIMP-2, and explains why our activation experiments yield identical results for these two mutants.

The activation experiments from the transient transfection of the *TIMP-2*$^{-/-}$ cells were further analysed for the distribution of the TIMPs in lysates and medium (Figure 5, bottom panel, all Western blots). As expected, transfection with wild-type TIMP-2 allowed activation of proMMP-2 to the intermediate and fully active form, while the IQ-TIMP-2 and N-TIMP-4:C-TIMP-2 mutant allowed processing to the intermediate form (Figure 5, bottom panel, zymogram). Western blot analysis revealed that wild-type TIMP-2, IQ-TIMP-2 and the N-TIMP-4:C-TIMP-2 mutants were present in both lysates and medium (Figure 5, bottom panel, Western blots, lanes 3, 4 and 5, respectively), suggesting that they are bound to cell-surface-associated MT1-MMP to some degree. In contrast, TIMP-4 was only detected in the medium (Figure 5, bottom panel, lane 6), suggesting that the amounts of TIMP-4 bound to MT1-MMP may be below the detection limit of our antibody, which was confirmed using reverse zymography (results not shown). Attempts to identify MT-1 MMP-bound TIMP-4 by immunolocalization showed only 1–2 % positively stained cells (results not shown), although appropriate control experiments with TIMP-2 showed strong cell-surface-staining with ≈ 15–20 % positive cells. This indicated that TIMP-4 levels were rather low and possibly below the detection limit of our antibody directed against the N-terminal domain of TIMP-4.

DISCUSSION

ProMMP-2 activation by cell-surface-associated MT1-MMP is dependent on the establishment of a 'receptor' comprised of MT1-MMP and TIMP-2, which allows binding of proMMP-2, via C-terminal domain interactions, to the inhibitor. Subsequent processing of proMMP-2 by an adjacent inhibitor-free MT1-MMP molecule proceeds by autoproteolytic conversion into active MMP-2 *in vitro* and *in vivo* [21,22]. It was the purpose of this study to identify the TIMP-2 domains and sequence motifs that govern proMMP-2 binding and activation by MT1-MMP in a TIMP-2-free environment. This approach allowed us to define the domain and detailed sequence requirements for this unique activation mechanism at the molecular level.

For this purpose, we developed stable cell lines overexpressing MT1-MMP in *TIMP-2*$^{-/-}$ cells and established an efficient refolding protocol to produce recombinant full-length TIMP-4 and TIMP-4 domain mutants. The full-length wild-type and mutant TIMP-4 proteins were shown to bind both wild-type proMMP-2 and proE^{375} → A MMP-2 and inhibited catMT1-MMP, thereby indicating structural integrity of both N- and C-terminal domains.

Analysis of bimolecular complex formation with proMMP-2 C-terminal domain SL chimaeric mutants showed that only one mutant formed a proenzyme–TIMP-4 complex (proMMP-2-C-SLGLGL), while the other two mutants were inactive. Indeed we speculated from the detailed analyses of the C-terminal MMP-2-binding site for TIMP-2 [37] that the positively charged cluster (K^{558}, K^{610}, K^{617} and R^{561}) on MMP-2 would also be important for bimolecular complex formation with TIMP-4. Subsequently our data confirmed that the binding site for TIMP-4 to proMMP-2 mapped to this positively charged cluster as it is localized in blades 3 and 4 of the haemopexin-like C-terminal domain of proMMP-2 that is present in proMMP-2-C-SLGLGL [24,29]. This part of MMP-2 contains two hydrophobic pockets that make direct contact with the C-terminal domain of TIMP-2, which are additionally flanked by electrostatic interactions and hydrogen bonds [24]. The X-ray data of the TIMP-2–proMMP-2 complex confirmed that the K^{620} and K^{610} residues of proMMP-2 form a double positive cluster that interacts with Y^{139} on TIMP-2, which had been identified earlier by mutagenesis to be important for the bimolecular complex formation [37]. From the crystal structural data of the TIMP-2–proMMP-2 complex we can deduce that the C-terminal interactions within a TIMP-4–proMMP-2 complex are considerably weaker [24]. This is due to the lack of the hydrogen bond between T^{153}–Y^{607} and the salt bridge of R^{170}–L^{616}, as these residues are L^{154} and H^{171} in TIMP-4. Furthermore, a reduction of hydrophobic interactions at the centre of the pocket is also obvious, since M^{149} in TIMP-2 is replaced by T^{150}, a more hydrophilic amino acid in TIMP-4. The X-ray structural analysis also revealed important interactions between the tail sequence of TIMP-2 and proMMP-2, which are mainly electrostatic in nature [24]. These are R^{179}–D^{586}, K^{185}–D^{579}, E^{187}–K^{547}, D^{190}–R^{561} and E^{192}–K^{566}. Only three of these five salt bridges are completely conserved in TIMP-4. Although it is possible that R^{186} in TIMP-4 could establish a salt bridge with D^{579}, this interaction would presumably be less favourable due to the size difference between K^{185} and R^{186}. Therefore a bimolecular complex between TIMP-4 and proMMP-2 would be considerably less stable than the corresponding TIMP-2–proMMP-2 complex since important amino acid residues at the interaction interface are not conserved across these TIMPs. This is in agreement with our data and was also shown by elegant displacement experiments by Bigg et al. [14], where TIMP-2 displaced TIMP-4 from a proMMP-2–TIMP-4 complex.

Subsequent kinetic analysis of catMT1-MMP inhibition demonstrated that full-length TIMP-4 was strongly dependent on C-terminal domain interactions between the inhibitor and catMT1-MMP, with apparent K_i values below ≈ 3–2 pM. These values can only be regarded as a rough estimate of the true value, due to the limitations of the assay sensitivity, which did not allow us to perform these experiments at enzyme concentrations at or below the K_i [34]. These values are considerably lower than those published recently [14] and may reflect differences in the experimental set up, since our experiments were performed using longer pre-incubation periods prior to analysis at 25 °C. Additionally, our k_{on} values reported here for the interaction between catMT1-MMP and TIMP-4 vary by an order of magnitude from the values published for a transmembrane

© 2003 Biochemical Society

deletion mutant of MT1-MMP [14], which may reflect C-terminal domain interaction between the C-terminal domain of MT1-MMP and TIMP-4 or indeed species differences between murine TIMP-4 used here and human TIMP-4. Unexpectedly, the apparent K_i for the proE^{375} → A MMP-2–TIMP-4 complex was nearly identical with that of full-length TIMP-4. We had predicted that the apparent K_i for the proE^{375} → A MMP-2–TIMP-4 complex would considerably increase, due to steric hindrance from the bound proE^{375} → A MMP-2. However, our experiments show that this was not the case within the experimental limits of our analysis. We concluded that proE^{375} → A MMP-2 possibly dissociated from the C-terminal domain of TIMP-4 following docking of catMT1-MMP to the N-terminal domain of the inhibitor. This was confirmed by our analysis of trimolecular complex formation, which showed that TIMP-4 dissociated from proE^{375} → A MMP-2 in the presence of catMT1-MMP. Our data predicted that wild-type TIMP-4 would be unable to support proMMP-2 binding to a putative 'MT1-MMP/TIMP-4 receptor' at the cell surface and that proMMP-2 activation would be impaired. This was confirmed here experimentally, using *TIMP-2*$^{-/-}$ cells transfected with MT1-MMP, and by others [14,16].

Analysis of trimolecular complex formation between TIMP-4 mutants, proE^{375} → A MMP-2 and catMT1-MMP provided an important insight into the domain and detailed sequence requirements of TIMP-2 as a determinant for proMMP-2 activation at the cell surface. This approach demonstrated that wild-type TIMP-4 was unable to support stable trimolecular complex formation with catMT1-MMP and proE^{375} → A MMP-2. In contrast, the chimaeric inhibitors N-TIMP-4:C-TIMP-2, as well as the TIMP-4:TIMP-2 tail mutants TIMP-4:TIMP-2$^{K185-P194}$ and TIMP-4:TIMP-2$^{E192-D193}$, were able to bind both catMT1-MMP and proE^{375} → A MMP-2. Thus the introduction of a single salt bridge (E^{192}–K^{566}) in the tail mutant TIMP-4:TIMP-2$^{E192-D193}$ was sufficient to provide trimolecular complex formation capability between the inhibitor, catMT1-MMP and proMMP-2. Additionally, the TIMP-2 tail-deletion mutant $\Delta_{186-194}$TIMP-2 failed to establish a stable trimolecular complex with proE^{375} → A MMP-2 and catMT1-MMP (results not shown), which is due to the loss of three electrostatic interactions between E^{187}, D^{190} and E^{192} of TIMP-2 and K^{547}, R^{561} and K^{566} of proMMP-2 [24]. From our analyses of the stability of trimolecular complexes between proE^{375} → A MMP-2, the TIMP-4 mutants and catMT1-MMP we can conclude that the charged tail sequence of TIMP-2 (E^{192}–D^{193}) contributes considerably to their stability. This has been confirmed by the identified interactions of the charged tail of TIMP-2 with proMMP-2, which are only partially conserved in TIMP-4 [24]. In detail the loss of E^{192} and D^{193} does result in an impairment of trimolecular complex formation. These residues were also identified by Kai et al. [39] as major contributors to the stability of the TIMP-2–proMMP-2 complex, using a C-terminal myoglobin-fusion-protein approach.

ProMMP-2 activation by MT1-MMP in *TIMP-2*$^{-/-}$ cells demonstrated that the chimaeric inhibitor N-TIMP-4:C-TIMP-2 induced processing of proMMP-2 to the intermediate form, while N-TIMP-2:C-TIMP-4 and wild-type TIMP-4 were completely inactive. The processing to the intermediate form of proMMP-2 can occur in the absence of TIMP-2 when concanavalin A is used in experimental model systems to stabilize artificially high MT1-MMP levels at the cell surface [21,22]. However, our cell system only showed conversion into the intermediate or indeed fully active form when the appropriate amounts of wild-type or TIMP mutants were present. Although TIMP-4 represents a potent MT1-MMP inhibitor showing an apparent K_i value below 2 pM, we had problems demonstrating that this inhibitor bound to cell-surface-associated MT1-MMP using both immunocytochemistry and Western blot analysis of cell lysates in our *TIMP-2*$^{-/-}$-derived cellular model system and this may be due to the lack of high-affinity TIMP-4 antibodies. Our k_{on} data for the association rate constant of complex formation between catMT1-MMP and TIMP-4 showed that is was an order of magnitude lower than TIMP-2, indicating that the N-terminal domain interactions between MT1-MMP and TIMP-4 are less favourable. However, our data contrast with those published by Bigg et al. [14], which reported that the association rate constant was higher for TIMP-4 than TIMP-2 for the interaction with a transmembrane deletion mutant of MT1-MMP. We cannot, however, confirm these results as analysis of a transmembrane deletion mutant of MT1-MMP with our murine TIMP-4 preparations revealed identical results to those observed with catMT1-MMP (M. Rapti, R. Williamson, M. H. Lee, V. Knäuper and G. Murphy, unpublished work) and we therefore believe that the murine TIMP-4 association rate is an order of magnitude lower than that of human TIMP-2. This could be in part due to the difference in the AB loop structure of the two TIMPs, which we had identified earlier to be an important determinant of the MT1-MMP–TIMP-2 interaction [25] and the lack of Y^{36} in TIMP-4. In contrast, N-TIMP-4:C-TIMP-2 was identified in cell lysates of MT1-MMP-transfected cells from the *TIMP-2*$^{-/-}$ mouse, leading us to conclude that the C-terminal domain of TIMP-2 is playing an important role in cell-surface association of the inhibitor.

The importance of the TIMP-2 tail-sequence motifs in proMMP-2 activation by MT1-MMP was further underlined using the tail-deletion mutant $\Delta_{186-194}$TIMP-2 since it was unable to promote proMMP-2 activation by MT1-MMP at the cell surface. The loss of three salt bridges across the proMMP-2–TIMP-2 interaction interface rendered the tail-deletion mutant $\Delta_{186-194}$TIMP-2 inactive [24]. We demonstrated that two amino acid residues of the TIMP-2 tail sequence were important for this unique ability of TIMP-2 to mediate proMMP-2 activation by MT1-MMP at the cell surface, since the IQ-TIMP-2 mutant showed impaired activation capability. This mutant has only lost a single salt bridge (E^{192}–K^{566}) at the proMMP-2–TIMP-2 interface, and this loss is sufficient to impair proMMP-2 activation at the cell surface considerably [24]. In conclusion, our data have therefore identified the charged amino acid residues E^{192}–D^{193} within the TIMP-2 tail sequence as a major determinant for the establishment of the MT1-MMP/TIMP-2 'receptor', which allows proMMP-2 activation at the cell surface by MT1-MMP.

It is clear that TIMP-2 has unique relationships with both MT1-MMP and proMMP-2, and these relationships have evolved to fulfil its unique role in the activation of the latter by the former at the cell surface. This mechanism is utilized by cancer cells, allowing focal degradation of the extracellular matrix surrounding the tumour, which may be regarded as a trigger event for cell protrusion, migration and invasion, ultimately resulting in the establishment of metastases in distant organs. The data presented within this report have identified important amino acid residues in TIMP-2 that facilitate the unique mechanism of proMMP-2 activation by MT1-MMP. They form the basis for engineering TIMP-2 mutants that will efficiently block MT1-MMP-driven activation of proMMP-2, and these inhibitors will represent important novel tools in gene-therapeutic approaches to suppress tumour invasion and metastases in the future.

We thank Peter Loader for technical assistance during the initiation of the project, and Dr Rosalind Hembry for the immunization of a sheep with N-TIMP-4 and help with confocal microscopy. This work was supported by grants from the British Heart Foundation, the Wellcome Trust, the Nuffield Foundation, the Arthritis Research Campaign and the Biotechnology and Biological Sciences Research Council.

© 2003 Biochemical Society

REFERENCES

1 Nagase, H. and Woessner, J. F. (2000) Matrix metalloproteinases. J. Biol. Chem. **274**, 21491–21494
2 Edwards, D. R. and Murphy, G. (1998) Cancer – proteases – invasion and more. Nature (London) **394**, 527–528
3 Itoh, T., Tanioka, M., Yoshida, H., Yoshioka, T., Nishimoto, H. and Itohara, S. (1998) Reduced angiogenesis and tumor progression in gelatinase A-deficient mice. Cancer Res. **58**, 1048–1051
4 Zhou, Z. J., Apte, S. S., Soininen, R., Cao, R. H., Baaklini, G. Y., Rauser, R. W., Wang, J. M., Cao, Y. H. and Tryggvason, K. (2000) Impaired endochondral ossification and angiogenesis in mice deficient in membrane-type matrix metalloproteinase I. Proc. Natl. Acad. Sci. U.S.A. **97**, 4052–4057
5 Baker, A. H., Ahonen, M. and Kahari, V. M. (2000) Potential applications of tissue inhibitor of metalloproteinase (TIMP) overexpression for cancer gene therapy. Adv. Exp. Med. Biol. **465**, 469–483
6 Docherty, A. J., Lyons, A., Smith, B. J., Wright, E. M., Stephens, P. E., Harris, T. J., Murphy, G. and Reynolds, J. J. (1985) Sequence of human tissue inhibitor of metalloproteinases and its identity to erythroid-potentiating activity. Nature (London) **318**, 66–69
7 Apte, S. S., Mattei, M.-G. and Olsen, B. R. (1994) Cloning of the cDNA encoding human tissue inhibitor of metalloproteinases-3 (TIMP-3) and mapping of the TIMP3 gene to chromosome 22. Genomics **19**, 86–90
8 Greene, J., Wang, M. S., Liu, Y. L. E., Raymond, L. A., Rosen, C. and Shi, Y. N. E. (1996) Molecular cloning and characterization of human tissue inhibitor of metalloproteinase 4. J. Biol. Chem. **271**, 30375–30380
9 Boone, T. C., Johnson, M. J., De Clerck, Y. A. and Langley, K. E. (1990) cDNA cloning and expression of a metalloproteinase inhibitor related to tissue inhibitor of metalloproteinases. Proc. Natl. Acad. Sci. U.S.A. **87**, 2800–2804
10 Brew, K., Dinakarpandian, D. and Nagase, H. (2000) Tissue inhibitors of metalloproteinases: evolution, structure and function (1). Biochim. Biophys. Acta **1477**, 267–283
11 Butler, G. S., Will, H., Atkinson, S. J. and Murphy, G. (1997) Membrane-type-2 matrix metalloproteinase can initiate the processing of progelatinase A and is regulated by the tissue inhibitors of metalloproteinases. Eur. J. Biochem. **244**, 653–657
12 Liu, Y. E., Wang, M., Greene, J., Su, J., Ullrich, S., Li, H., Sheng, S., Alexander, P., Sang, Q. A. and Shi, Y. E. (1997) Preparation and characterisation of recombinant tissue inhibitor of metalloproteinase 4 (TIMP-4). J. Biol. Chem. **272**, 20479–20483
13 Bigg, H. F., Shi, Y. E., Liu, Y. E., Steffensen, B. and Overall, C. M. (1997) Specific, high affinity binding of tissue inhibitor of metalloproteinases-4 (TIMP-4) to the COOH-terminal hemopexin-like domain of human gelatinase A. J. Biol. Chem. **272**, 15496–15500
14 Bigg, H. F., Morrison, C. J., Butler, G. S., Bogoyevitch, M. A., Wang, Z., Soloway, P. D. and Overall, C. M. (2001) Tissue inhibitor of metalloproteinases-4 inhibits but does not support the activation of gelatinase A via efficient inhibition of membrane type 1-matrix metalloproteinase. Cancer Res. **61**, 3610–3618
15 Morrison, C. J., Butler, G. S., Bigg, H. F., Roberts, C. R., Soloway, P. D. and Overall, C. M. (2001) Cellular activation of MMP-2 (gelatinase A) by MT2-MMP occurs via a TIMP-2-independent pathway. J. Biol. Chem. **276**, 47402–47410
16 Hernandez-Barrantes, S., Shimura, Y., Soloway, P. D., Sang, Q. A. and Fridman, R. (2001) Differential roles of TIMP-4 and TIMP-2 in Pro-MMP-2 activation by MT1-MMP. Biochem. Biophys. Res. Commun. **281**, 126–130
17 Strongin, A. Y., Collier, I., Bannikov, G., Marmer, B. L., Grant, G. A. and Goldberg, G. I. (1995) Mechanism of cell surface activation of 72-kDa type IV collagenase. Isolation of the activated form of the membrane metalloprotease. J. Biol. Chem. **270**, 5331–5338
18 Hernandez-Barrantes, S., Toth, M., Bernardo, M. M., Yurkova, M., Gervasi, D. C., Raz, Y., Sang, Q. A. and Fridman, R. (2000) Binding of active (57 kDa) membrane type 1-matrix metalloproteinase (MT1-MMP) to tissue inhibitor of metalloproteinase (TIMP)-2 regulates MT1-MMP processing and pro-MMP-2 activation. J. Biol. Chem. **275**, 12080–12089
19 Atkinson, S. J., Crabbe, T., Cowell, S., Ward, R. V., Butler, M. J., Sato, H., Seiki, M., Reynolds, J. J. and Murphy, G. (1995) Intermolecular autolytic cleavage can contribute to the activation of progelatinase A by cell membranes. J. Biol. Chem. **270**, 30479–30485
20 Sato, H., Takino, T., Okada, Y., Cao, J., Shinagawa, A., Yamamoto, E. and Seiki, M. (1994) A matrix metalloproteinase expressed on the surface of invasive tumour cells. Nature (London) **370**, 61–65
21 Wang, Z., Juttermann, R. and Soloway, P. D. (2000) TIMP-2 is required for efficient activation of proMMP-2 in vivo. J. Biol. Chem. **275**, 26411–26415
22 Caterina, J. J., Yamada, S., Caterina, N. C., Longenecker, G., Holmback, K., Shi, J., Yermovsky, A. E., Engler, J. A. and Birkedal-Hansen, H. (2000) Inactivating mutation of the mouse tissue inhibitor of metalloproteinases-2(Timp-2) gene alters proMMP-2 activation. J. Biol. Chem. **275**, 26416–26422
23 Willenbrock, F., Crabbe, T., Slocombe, P. M., Sutton, C. W., Docherty, A. J. P., Cockett, M. I., O'Shea, M., Brocklehurst, K., Phillips, I. R. and Murphy, G. (1993) The activity of the tissue inhibitors of metalloproteinases is regulated by C-terminal domain interactions: a kinetic analysis of the inhibition of gelatinase A. Biochemistry **32**, 4330–4337
24 Morgunova, E., Tuuttila, A., Bergmann, U. and Tryggvason, K. (2002) Structural insight into the complex formation of latent matrix metalloproteinase 2 with tissue inhibitor of metalloproteinase 2. Proc. Natl. Acad. Sci. U.S.A. **99**, 7414–7419
25 Butler, G. S., Hutton, M., Wattam, B. A., Williamson, R. A., Knäuper, V., Willenbrock, F. and Murphy, G. (1999) The specificity of TIMP-2 for matrix metalloproteinases can be modified by single amino acid mutations. J. Biol. Chem. **274**, 20391–20396
26 Williamson, R. A., Natalia, D., Gee, C. K., Murphy, G., Carr, M. D. and Freedman, R. B. (1996) Chemically and conformationally authentic active domain of human tissue inhibitor of metalloproteinases-2 refolded from bacterial inclusion bodies. Eur. J. Biochem. **241**, 476–483
27 Williamson, R. A., Bartels, H., Murphy, G. and Freedman, R. B. (1994) Folding and stability of the active N-terminal domain of tissue inhibitor of metalloproteinases-1 and -2. Protein Eng. **7**, 1035–1040
28 Hembry, R. M., Murphy, G. and Reynolds, J. J. (1985) Immunolocalization of tissue inhibitor of metalloproteinases (TIMP) in human cells. Characterization and use of a specific antiserum. J. Cell Sci. **73**, 105–119
29 Butler, G. S., Butler, M. J., Atkinson, S. J., Will, H., Tamura, T., Van Westrum, S. S., Crabbe, T., Clements, J., D'Ortho, M.-P. and Murphy, G. (1998) The TIMP2 membrane type 1 metalloproteinase "receptor" regulates the concentration and efficient activation of progelatinase A. J. Biol. Chem. **273**, 871–880
30 Crabbe, T., Zucker, S., Cockett, M. I., Willenbrock, F., Tickle, S., O'Connell, J. P., Scothern, J. M., Murphy, G. and Docherty, A. J. P. (1994) Mutation of the active site glutamic acid of human gelatinase A: effects on latency, catalysis, and the binding of tissue inhibitor of metalloproteinases-1. Biochemistry **33**, 6684–6690
31 Balbín, M., Fueyo, A., Knäuper, V., Pendás, A. M., López, J. M., Jiménez, M. G., Murphy, G. and López-Otín, C. (1998) Collagenase 2 (MMP-8) expression in murine tissue-remodeling processes – analysis of its potential role in postpartum involution of the uterus. J. Biol. Chem. **273**, 23959–23968
32 D'Ortho, M.-P., Stanton, H., Butler, M., Atkinson, S. J., Murphy, G. and Hembry, R. M. (1998) MT1-MMP on the cell surface causes focal degradation of gelatin films. FEBS Lett. **421**, 159–164
33 Murphy, G. and Willenbrock, F. (1995) Tissue inhibitors of matrix metalloendopeptidases. Methods Enzymol. **248**, 496–510
34 Hutton, M., Willenbrock, F., Brocklehurst, K. and Murphy, G. (1998) Kinetic analysis of the mechanism of interaction of full-length TIMP-2 and gelatinase A: evidence for the existence of a low-affinity intermediate. Biochemistry **37**, 10094–10098
35 Knight, C. G., Willenbrock, F. and Murphy, G. (1992) A novel coumarin-labelled peptide for sensitive continuous assays of the matrix metalloproteinases. FEBS Lett. **296**, 263–266
36 Ward, R. V., Atkinson, S. J., Slocombe, P. M., Docherty, A. J. P., Reynolds, J. J. and Murphy, G. (1991) Tissue inhibitor of metalloproteinases-2 inhibits the activation of 72 kDa progelatinase by fibroblast membranes. Biochim. Biophys. Acta **1079**, 242–246
37 Overall, C. M., King, A. E., Sam, D. K., Ong, A. D., Lau, T. Y., Wallon, U. M., DeClerck, Y. A. and Atherstone, J. (1999) Identification of the tissue inhibitor of metalloproteinases-2 (TIMP-2) binding site on the hemopexin carboxyl domain of human gelatinase A by site-directed mutagenesis. The hierarchical role in binding TIMP-2 of the unique cationic clusters of hemopexin modules iii and iv. J. Biol. Chem. **274**, 4421–4429
38 Toth, M., Bernardo, M. M., Gervasi, D. C., Soloway, P. D., Wang, Z., Bigg, H. F., Overall, C. M., DeClerck, Y. A., Tschesche, H., Cher, M. L. et al. (2000) TIMP-2 acts synergistically with synthetic MMP inhibitors but not with TIMP-4 to enhance the MT1-MMP-dependent activation of Pro-MMP-2. J. Biol. Chem. **275**, 41415–41423
39 Kai, H. S., Butler, G. S., Morrison, C. J., King, A. E., Pelman, G. R. and Overall, C. M. (2002) Utilization of a novel recombinant myoglobin fusion protein expression system to characterize the TIMP-4 and TIMP-2 C-terminal domain and tails by mutagenesis: the importance of acidic residues in binding the MMP-2 hemopexin C domain. J. Biol. Chem. **277**, 48696–48707

Received 8 October 2002/21 February 2003; accepted 12 March 2003
Published as BJ Immediate Publication 12 March 2003, DOI 10.1042/BJ20021573

© 2003 Biochemical Society